Construction and Building Materials 48 (2013) 210–217

Contents lists available at SciVerse ScienceDirect

Construction and Building Materials

journal homepage: www.elsevier.com/locate/conbuildmat

# Using image analysis to measure the porosity distribution of a porous pavement

William D. Martin III *, Bradley J. Putman, Nigel B. Kaye

*Glenn Department of Civil Engineering, Clemson University, Clemson, SC 29634, USA*

## HIGHLIGHTS

- A method for measuring porosity distributions using image analysis was developed.
- Average porosity measured by image analysis was comparable to volumetric methods.
- Standardization of the representative elemental area (REA) calculation was proposed.
- A conservative REA was found to be 83.9 $cm^2$ for the gradations tested.
- The vertical porosity distribution from image analysis agrees with previous models.

## ARTICLE INFO

*Article history:*
Received 9 May 2013
Received in revised form 21 June 2013
Accepted 27 June 2013
Available online 27 July 2013

*Keywords:*
Porous pavement
Porosity
Image analysis
Representative elemental area

## ABSTRACT

A method for determining the distribution of porosity across a porous pavement sample using image analysis was developed and evaluated. Its measured average porosity compares favorably to other porosity methods including two volumetric based methods and ASTM D7063 which uses a vacuum sealing device. The impact of the representative elemental area (REA), which is the minimum pavement cross sectional area that must be analyzed to have a statistically significant measure of the pavement porosity, was investigated. The REA was experimentally determined to be 83.9 $cm^2$ (13 $in.^2$) for the different gradations of porous pavements evaluated, which were ASTM standard gradations No. 89, No. 78, No. 7, and No. 67. Though this method can be used to measure a one dimensional porosity distribution in different directions (vertically, horizontally, or radially in cylinders), this work focused on its application to vertical porosity distributions. Using the results of the image analysis and the REA, a smoothed profile of the porosity distribution was produced which showed that, for a porous pavement sample compacted in a single lift, the porosity is high at the surface, due to the surface texture, decreases drastically to a minimum at approximately 2–3 cm (~1 in.) in depth and then linearly increases until approximately two centimeters from the bottom of the sample where the porosity increases drastically due to the wall effects. The porosity distribution produced agrees with previously proposed distributions.



## 1. Introduction

This paper presents a method to measure the porosity distribution in a porous pavement. Porosity is critical to the hydraulic functionality of a pavement which is why studies have been conducted that look at the relationship between porosity and hydraulic conductivity; however, most of these studies use or assume homogenous samples [1–5]. When the porosity has a non-homogenous distribution, especially in the vertical direction, the average porosity may vary greatly from the porosity of the limiting layer which strongly influences the hydraulic conductivity. This has practical importance because over-consolidation and surface sealing are common problems associated with improperly constructed pervious concrete pavements [6]. In these situations, the average porosity of a core may be acceptable by the specifications, while the hydraulic conductivity, which is limited by the low porosity layer, is not.

Additionally, the vertical porosity distribution influences the filtering and clogging capabilities of the pavement. Studies have found that clogging of pavements occurs at two locations which are determined by particle size [7]. Large particles, like sand, tend to get trapped on the surface of the pavement while smaller particles, like clay, travel through the pavement and build up on the subsoil or filter fabric below. The presence of a vertical porosity distribution can greatly impact this behavior and could be manipulated to make the filtering more effective.

Prior studies have attempted to measure this porosity distribution with other methods. One of the first, by De Somer and De

* Corresponding author. Address: 109 Lowry Hall, Clemson, SC 29634, USA. Tel.: +1 (864) 245 5046; fax: +1 (864) 656 2670.
*E-mail address:* wmartin@g.clemson.edu (W.D. Martin III).

0950-0618/$ - see front matter © 2013 Elsevier Ltd. All rights reserved.
http://dx.doi.org/10.1016/j.conbuildmat.2013.06.093

Winne [8], did this by incrementally adding a known volume of water to a container in which a porous specimen was hanging. The relationship between the volume of water added and the change in height of the water level allowed a porosity value to be found at incremental distances along the height of the specimen. However, De Somer and De Winne [8] reported some problems with this method. The capillary action of the water caused extra water to be taken up by the sample which makes the porosity appear greater at that point than it actually is. Also, when the sample is slowly submerged, some pores entrap air that would be released when using other porosity testing methods, which could lower the measured porosity values. This problem would be exacerbated when the porosity is low. Even with these shortcomings, their results for the nine samples tested show a similar pattern of having a slightly lower porosity near the surface (due to the slight compaction which results from surface smoothing) followed by a slight increase in porosity in the middle which then decreased approaching the bottom. The researchers attribute this pattern to using vibration as the compaction method. The vibration caused the lower viscosity cement paste to flow down towards the bottom of the sample, increasing the upper porosity and decreasing the lower [8].

When tamping is used as a compaction method, a different pattern in the porosity distribution is observed. Haselbach and Freeman [9] used samples that had been surface compacted in the field and found that the top quarter of the pavement had a much lower porosity than the middle half of the sample, with the lowest quarter having the greatest porosity. Their technique for looking at the vertical porosity distribution produced a much coarser profile than De Somer and De Winne's [8]. They simply split the cores into the top and bottom quarter and the middle half, and used common volumetric porosity methods to measure the individual pieces. These three data points were then used to create the profile.

The objective of this study was to develop a method to measure the porosity distribution of a porous pavement sample using an image analysis method which has been used by other researchers to find material properties such as average porosity and pore size distribution [10–12]. This method provides a much better resolution of the porosity distribution than Haselbach and Freeman's [9] method while avoiding some of the measurement technique drawbacks encountered by De Somer and De Winne [8]. While this method can be used to measure the porosity distribution in any direction, this paper focuses on vertical porosity distribution because of its importance to the hydraulic behavior in porous pavements.

## 2. Materials and methods

### 2.1. Mix design

Four pervious concrete mixes using different gradations [13] were used to develop and calibrate the image analysis method in addition to cores taken from a pavement installation. Twelve compacted cylinders were made from each of the four mixes shown in Table 1; six were used to find the vertical porosity distribution using image analysis and the other six to find the porosity profile using volumetric testing of 2.5 cm (1 in.) slices, similar to Haselbach and Freeman [9].

Cylinders, 15.2 cm (6 in.) tall and 15.2 cm (6 in.) in diameter, were used because that is a common thickness of pervious concrete and simulating the porosity distribution over this height would closely approximate an over-consolidated pavement. Multiple studies have found that placing two layers and compacting each layer with 10 blows of the proctor hammer creates cylinders that replicate the average in situ properties of field placed concrete [14,15], but in the field, the specimen is only compacted in a single lift, which is the cause of the vertical porosity distribution. To replicate the surface compaction, the concrete was mixed and placed in one lift and was compacted with 20 blows of a standard proctor hammer.

When the first mix (VPD-89) was compacted the above compaction procedure was used. However, even though the mix was compacted in one lift, the mold did not have an extension collar as the specimen was compacted, so more concrete was added to the top to keep the mold as close to full as possible. This technique produced satisfactory surface compaction. However, it was found that adding a collar and initially overfilling the mold, so that no mix needed to be added during compaction, produced a more pronounced porosity distribution. Because this second compaction method is closer to field placement and exaggerates the porosity distribution, it was used for the other three mixes. Additionally, two cylinders from each mix were cast that had no compaction as a reference.

**Table 1**
Mix proportions and aggregate gradations used for four sets of pervious concrete samples.

| | Mix 1 (VPD-89) | Mix 2 (VPD-78) | Mix 3 (VPD-7) | Mix 4 (VPD-67) |
|---|---|---|---|---|
| Water/cement | 0.3 | 0.3 | 0.3 | 0.3 |
| Cement/aggregate | 0.25 | 0.28 | 0.28 | 0.28 |
| *Percent passing (%)* | | | | |
| 25 mm (1″) | 100 | 100 | 100 | 100 |
| 19 mm (3/4″) | 100 | 100 | 100 | 98 |
| 12.5 mm (1/2″) | 100 | 100 | 100 | 68 |
| 9.5 mm (3/8″) | 100 | 50 | 50 | 39 |
| 4.75 mm (#4) | 29 | 15 | 10 | 5 |
| 2.36 mm (#8) | 4 | 5 | 2 | 2 |
| 1.18 mm (#16) | 2 | 3 | – | – |
| 0.15 mm (#100) | 1 | – | – | – |

### 2.2. Volumetric porosity testing

To check the accuracy of the image analysis method when measuring total porosity, the porosity of a number of cores was measured using two volumetric methods and a vacuum sealing device to establish a baseline for the porosity [16,17]. The volumetric methods of measuring the porosity directly measure the volume, $V$, of the sample (based on an average of four measurements of the height and diameter) and weigh the sample both dry and submerged in water. In the first volumetric method the submerged weight is measured after soaking the cylinder for 30 min and tapping it to release any trapped air. The second applies a vacuum and vibration while the sample is submerged for a shorter period of time (5 min). Both the soaking and vacuum are used to release any trapped air from within the sample. The porosity, $\Phi$, is then found from the dry mass, $A$, and submerged mass, $D$, of the specimen using following equation [17]:

$$\Phi = \left(1 - \frac{A - D}{\rho_{H_2O} V}\right) \times 100 \tag{1}$$

where $\rho_{H_2O}$ is the density of water.

The vacuum sealing device uses another method to find the volume. The core is vacuum sealed inside a bag having a mass, $B$, and then weighed submerged underwater both sealed, $E$, and unsealed, $C$ [16]. The porosity is found as

$$\Phi = \frac{SG2 - SG1}{SG2} \times 100 \tag{2}$$

$$\text{Bulk Specific Gravity} = SG1 = \frac{A}{B - E - \frac{B-A}{F_T}} \tag{3}$$

$$\text{Apparent Specific Gravity} = SG2 = \frac{A}{B - C - \frac{B-A}{F_{T1}}} \tag{4}$$

where $F_T$ and $F_{T1}$ are the apparent specific gravity of the plastic sealing material when sealed and unsealed, respectively.

For the six cylinders which were cut up into 2.5 cm (1 in.) horizontal slices to measure the porosity distribution volumetrically (similar to Haselbach and Freeman [9]), all three volumetric methods were used on the first batch, VPD-89. However, because the methods' results were so similar, only the vacuum sealing method was used for the slices from the other three mixes.

### 2.3. Sample preparation for image analysis

To measure the vertical porosity of a pavement using image analysis, a cylinder or core was cut in half vertically through the middle. That provided a wide rectangular face that runs the length of the core. The cut face was painted with black spray paint to darken the pores of the sample. After drying, the cut surfaces were painted white with a broad tip (tip dimensions of 4 by 7 mm), opaque oil-based paint pen. Careful attention was taken to make sure this paint did not run onto the inside surfaces of the pores or into any very small pores. While care must be used during

painting, the process is repeatable as it is clear what areas should be painted and if white paint does get into a pore the sample can always be repainted. Fig. 1 shows pictures of one sample before and after painting.

### 2.4. Image acquisition and preparation

The specimen's face was scanned (using a transparency sheet as protection for the scanner glass) at high resolution (600 dpi). To further clean the image, a threshold value of 127 (RGB) was set using an open source photo editing software (GNU Image Manipulation Program [GIMP]) so that any pixels were either white (solid surface) or black (pore space) as in Fig. 2. The image was also cropped to just smaller than the borders of the sample's face. This was done to minimize the impact of the wall effect on the aggregate packing and because the edges of the face are prone to a loss of aggregate dislodged during cutting. For the 15.2 cm (6 in.) specimens, the width was set to 14.6 cm (5.75 in.).

### 2.5. Image analysis

To quantify the vertical pore distribution, the areal porosity (ratio of the area of the pores to the total area of the sample) for each row of pixels in the image was found using Matlab®. However, because a row of pixels is such a small area ($1.76 \times 10^{-5}$ cm$^2$ for the 14.6 cm (5.75 in.) wide, 600 dpi resolution images used), the resulting porosities have many fluctuations and are not a statistically accurate representation of the porosity of a horizontal slice of the material at that point. To smooth the fluctuations so that the porosity distribution is representative of the sample, the area used to find the porosity must be increased. However, the larger an area used, the less resolution the porosity distribution has. The smallest area that yields a representative porosity value for that location in the sample is called the representative elemental area (REA). This concept is parallel to that of a representative elemental volume (REV) [18], except that the porosity is being approximated by an area ratio in this case. The concept of an REA has been used before in a similar manner, for example when using thin soil sections for quantitative soil micromorphology [19]. It is important to note that the wider a sample is, the fewer pixel rows need to be averaged to reach a given REA. This means that using a wider sample (such as a 15.2 cm [6 in.] core) results in a vertical porosity distribution with a finer vertical spatial resolution than a vertical porosity distribution from a narrow sample (such as a 5.1 cm [2 in.] core) assuming the two samples have the same REA.

The recommendation for the REA presented by Sumanasooriya and Neithalath [12] (which they refer to as the representative area elements [RAE]) is simply that it needs to be much larger than the typical pore size. While this may be acceptable for finding average properties from an image, finding a porosity distribution requires that the REA be as small as possible (to provide maximum spatial resolution), while still being large enough to be representative of the local porosity.

#### 2.5.1. Representative elemental area (REA)

The simplest method to find the REA is to experimentally plot multiple data sets of the porosity versus area for a sample and find the point at which the data sets tend to converge. This data was generated by starting at randomly selected points on the image (using Matlab's random number function) and expanding an area from that point, measuring the porosity within the area at each increment. The number of points used is discussed in more detail in Section 3.2.1. To accommodate experimental variability in the sample, convergence was defined to be when the porosity values fell within a range of 5% centered on the average porosity of the sample. Fig. 3 shows the results using the image from Fig. 2, with the two horizontal lines representing the upper and lower bounds of the ±2.5% tolerance. The smallest area at which all the data lines stay within the tolerance is 22.7 cm$^2$ (8.9 in.$^2$), which can be taken as the REA for this sample.

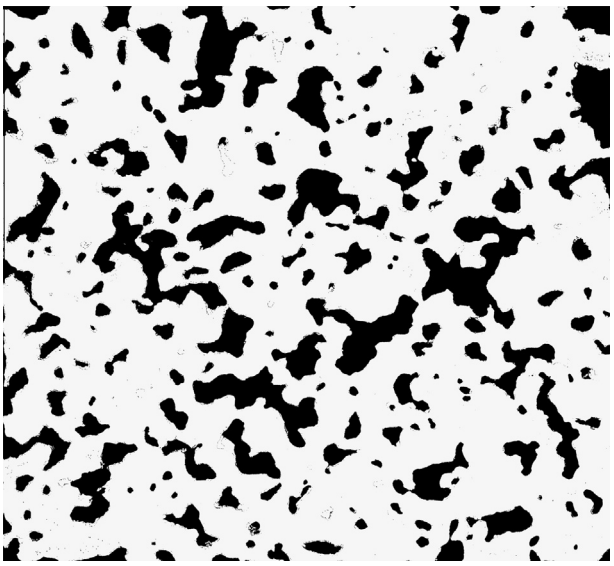

**Fig. 2.** Scanned and cleaned image of the core shown in Fig. 1 (pores are shown as black).

However, when the REA is being measured, there are three variables which are important: REA starting location, REA shape, and REA size. In Fig. 4, four areas, A–D, are selected from a well-packed distribution of circular particles to illustrate these considerations.

The starting location of the sample areas clearly has an impact on its porosity (compare areas A and B or C and D in Fig. 4) when the areas are small. As this area increases, the impact of starting locations should decrease for well-packed, spherical particles. However, the aggregates in porous pavements are far from spherical in their shape, and truly uniform samples are very difficult to create experimentally due to layering, compaction, and wall effects. Therefore, due to the small scale variability in a pavement, an experimentally measured REA may differ by location, even within a small sample. Fig. 3 is a prime example of this, where the three different starting locations produce a range of REA values from 0.5 to 22.7 cm$^2$ (0.2 to 8.9 in.$^2$).

The shape of the area used to calculate the REA can also influence the measurement. For well-packed particles, if a square (A or B in Fig. 4) is expanded, the resulting porosity quickly converges to the average porosity of the entire specimen. However, if a rectangle (C or D in Fig. 5) is expanded along its long axis, the average porosity of the specimen may never be reached. For the random structure of porous pavements which are more isotropic, this proves to be less of an issue. Bear [18] showed that the porosity found along a line (the length of the line that fell on voids divided by the total length of the line) should be representative of the volumetric porosity if the material is isotropic.

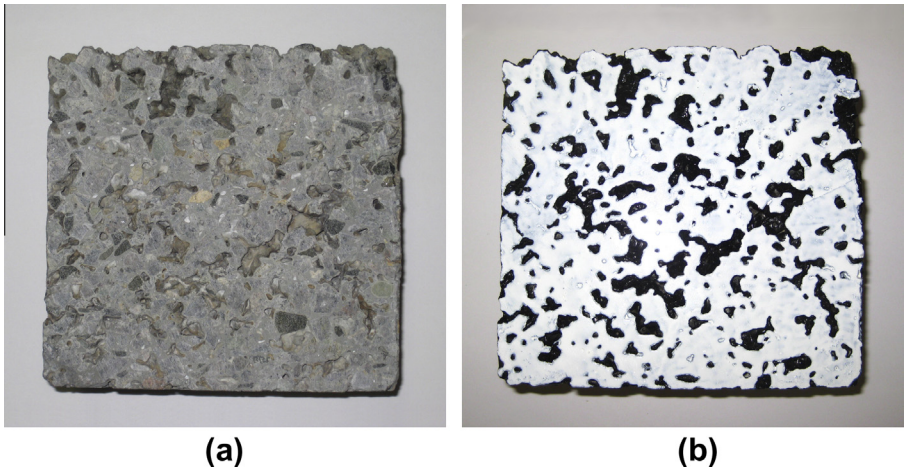


**Fig. 1.** Example of a 15.2 cm (6 in.) core (a) before and (b) after being painted.

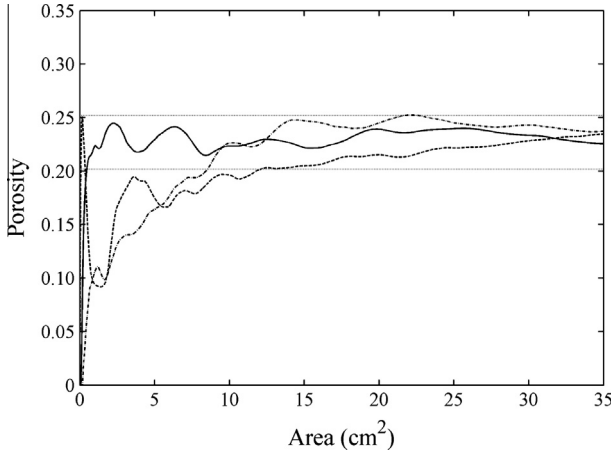


**Fig. 3.** Plot showing three of the porosity versus area data sets used to find the representative elemental area for the image from Fig. 2. The data falls completely within the ±2.5% tolerance when the area is greater than 22.7 cm$^2$ (8.9 in.$^2$).

The importance of size to the REA is inherent from its definition. The most variability in porosity occurs when the area is smaller than the average particle, and then decreases as the area grows (Fig. 3). The experimental range for REA values is determined in Section 3.2, along with the impact of the shape and number of starting locations.

It is important to note that the method above only works for a relatively homogenous sample as it relies on a measurement of the mean porosity of the sample to set the REA calibration limits. For a non-homogenous sample, this approach results in an REA that, by definition, is incapable of measuring porosity variations greater than 2.5%. The degree of non-uniformity on the smaller scale also affects the spread of the porosity, so the arbitrary choice of a 5% range may not be applicable for all cases.

*2.5.2. Vertical porosity profile smoothing using the REA*

Fig. 5 shows the porosity distribution found from the sample in Fig. 2. The single row porosity is the row by row calculation of the porosity and the smoothed porosity is the porosity calculated using a minimum area equal to the REA (22.7 cm$^2$ [8.9 in.$^2$]). Correlation between the bands of black (pore space) in the image, Fig. 2, and the high single row porosity can be seen. The smoothed porosity follows the trend of the single row porosity, but removes the extreme fluctuations. The average porosity calculated using image analysis, which represents the overall porosity for the sample, is given as a reference.

## 3. Results and discussion

### 3.1. Comparison of porosity methods

The average porosity of the full samples found using the image analysis method was compared to the three independent measures

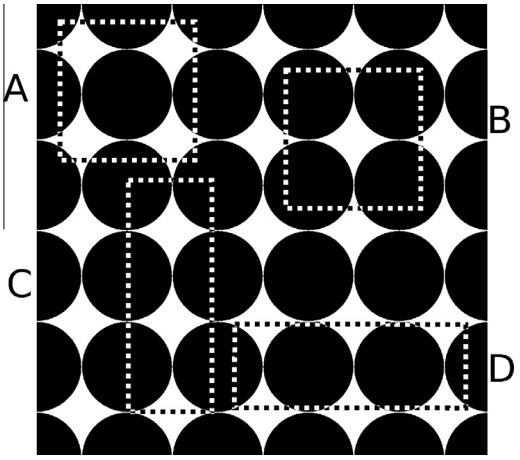


**Fig. 4.** Four areas, A–D, which demonstrate the effect of location, shape, and size of area on the REA.

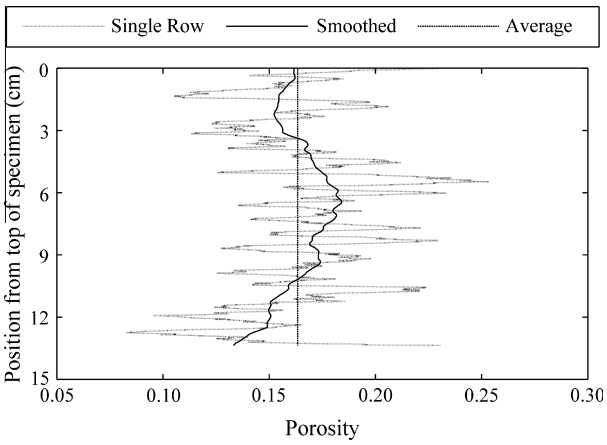


**Fig. 5.** Plot of the vertical porosity distribution of from the sample core shown in Fig. 1 with single row, smoothed, and average porosity, from image analysis. An REA of 22.7 cm$^2$ (8.9 in.$^2$).was used for the smoothing.

of porosity. The vacuum method was not used for the VPD-89 samples because a testing bowl tall enough to test a full cylinder had not been fabricated at that point in testing. Fig. 6 clearly shows that the vacuum sealing method gives the lowest porosity measurement followed by the soaking, vacuum, and image analysis methods in that order.

Using an ANOVA test, it was found that at least one of the methods was statistically different from the others ($\alpha = 0.05$). As a follow up, paired *t*-tests were used to see which differences were statistically significant. Because the VPD-89 specimens were missing the vacuum porosity data, only VPD-78, 7 and 67 specimens were used for comparisons with the vacuum method. For the other comparisons all four mixes were used.

The results showed that of all the methods, only the image analysis and vacuum methods were not statistically different from one another. They were slightly larger than the other methods, though the variation between all the methods was small, being around 1–3%. These results agree with the results of other researchers which show that using image analysis to measure the porosity is comparable to other common methods [10,11].

Two possible reasons the image analysis method tends to yield a higher porosity could be from the difference between total and effective porosity in a specimen and knockout. Total porosity is a measure of all the pores in a specimen, while effective porosity includes only pores that are hydraulically accessible. For most porous

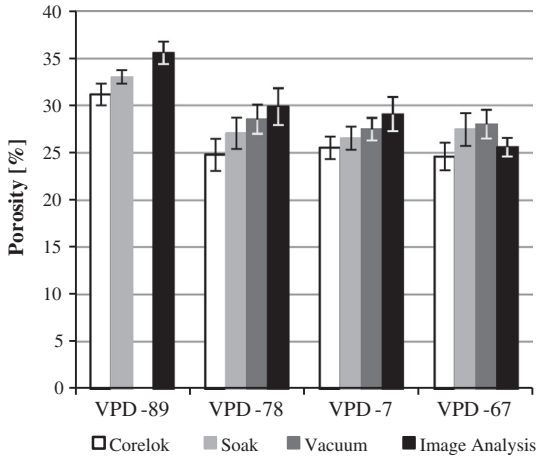


**Fig. 6.** Comparison of porosity measurement techniques.

pavements with an acceptable porosity (greater than 10–15%), effective and total porosity are very similar. However, as the volumetric porosity methods are measuring effective porosity and the image analysis method measures total porosity, any inaccessible voids present in the specimen could cause the image analysis method to be slightly higher.

The other probable cause of the increase in porosity is knockout, which is when small pieces of aggregate are knocked out of the sample during cutting or coring. It is common in porous pavements because there is less cementitious material to hold the aggregate particles in place. Haselbach and Freeman [20] found that knockout increased porosity by about 3% when comparing the porosity of a slab to that of numerous cores of the same slab. They proposed a correction factor to account for the knockout, but it is focused on the effects of knockout on volumetric porosity and does not apply directly to the image analysis calculation of porosity using a flat cut face. During the image preparation, the scanned face was cropped to remove the most severe impact of knockout (at the edges of the sample), but that does not entirely remove the impact of knockout on the specimen.

The impact of knockout was verified by taking the volumetric porosity of the individual horizontal slices and putting them together to find the average porosity for the whole cylinder such that

$$\Phi_{avg} = \frac{\sum_{slice=1}^{n} V_{slice}\Phi_{slice}}{\sum_{slice=1}^{n} V_{slice}} \quad (5)$$

The average porosity that is found is much closer to the image analysis porosity value which confirms the importance of knockout to the image analysis porosity measurement. These results for the VPD-89 specimens are given in Table 2.

### 3.2. Representative elemental areas (REA) for different aggregate gradations

#### 3.2.1. Required number of sampling locations for REA calculation

When using multiple, random starting locations to develop the porosity-area data set used to calculate the REA, as described in Section 2.5.1, the number of data sets used becomes important to the resulting REA value. The REA for a number of data sets combined is the largest of the individual data sets' REAs. Therefore, the more data sets used in calculation of the REA, the larger the resulting measured REA value becomes as it is more likely that one of the randomly selected starting locations is affected by non-uniformities and have a higher than average REA. Because of this, using more data sets also lowers the variability in the calculated REA. Fig. 7 shows this relationship graphically and the discussed trends are clearly visible. It appears that when using eight to ten data sets, the resulting REA becomes relatively constant as does the standard deviation.

From these results, it can be seen that, to get a good estimate for the REA of a sample, at least eight randomly located data sets need to be used. However, even with eight starting locations there is still some variability in the calculated REA. Repeating this procedure an additional seven times and taking the average of the eight REAs calculated ensures that the resulting REA is within 6.45 $cm^2$ (1 $in.^2$) of the actual REA with 95% confidence for the porous pavement samples tested in this study.

**Table 2**
Impact of knockout on average porosity values for mix VPD-89.

| | Average porosity (%) | | | |
|---|---|---|---|---|
| | Soak | Corelok | Vacuum | Image analysis |
| Cylinders | 33.4 | 31.1 | – | 35.6 |
| Slices | 36.4 | 35.1 | 36.1 | – |

#### 3.2.2. REA shape

To compare the effect of the shape of the area on the measurement of the REA, two shapes were tested. The first was a square which was expanded from an initial point evenly in all directions. The second was a rectangle the width of the image which was then expanded vertically from its initial position.

A comparison of the two shapes is shown in Fig. 8. Both methods used an acceptable variation of 5%. It can be seen that there is a reasonably strong correlation between the REAs found, though the square generally produced a larger REA. This is most likely because the square encounters local non-uniformity in both the vertical and horizontal directions, whereas the rectangle only encounters the vertical non-uniformities. Because the square produces a larger REA, which is more conservative, it is the better of the two shapes to use as expected.

#### 3.2.3. Calculation of experimental REA

Six specimens from each of the four mixes described in Section 2.1 were cut to create horizontal slices. Because the major porosity distribution in a cast cylinder is in the vertical direction, the cut faces of these slices were relatively uniform and had minimal porosity variation. Using the method in Section 2.5.1, the REA for each image was found eight times and the average value was taken as the REA for that image to ensure an accurate measurement. Because each sample from a mix can have a slightly different experimental REA, the experimental REA was measured for a number of horizontal slices from the samples. However, the horizontal slices were cut through areas with different porosities, due to the vertical porosity distribution, so the REA for each slice was plotted as a function of its porosity. Fig. 9 clearly illustrates that although there is a slight increasing trend between REA and porosity, the correlation is very low. The range of the REAs measured was between 23.1 and 91.7 $cm^2$ (3.58 and 14.22 $in.^2$).

One might expect that the REA would be strongly correlated to the porosity or particle size, however, the data in Fig. 9 shows that this is not the case. Those trends are on a smaller scale and the actual REA size is dominated by the larger scale non-uniformity of the mix which is affected by variables like the random shape of particles and the binder/paste distribution. The average and maximum values of REA for each gradation were found and plotted against the gradation's average aggregate size, $D_{50}$ (see Fig. 10). There is a slight increasing trend for the average REA, but it is not significant for the maximum REA values.

When choosing a standard REA to use for smoothing the porosity distribution data, it is better to use the maximum REA

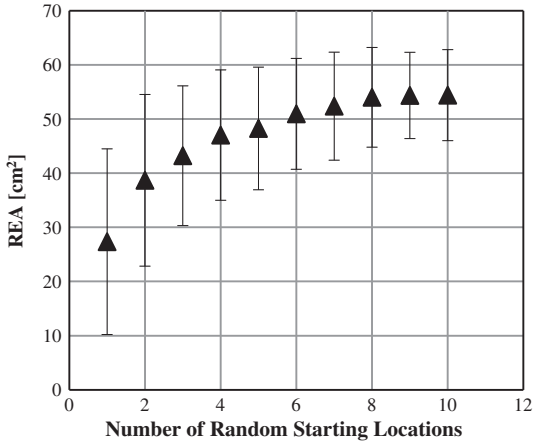


**Fig. 7.** Effect of increasing number of starting locations used to calculate the REA on the average REA (data points) and its standard deviation (error bars).

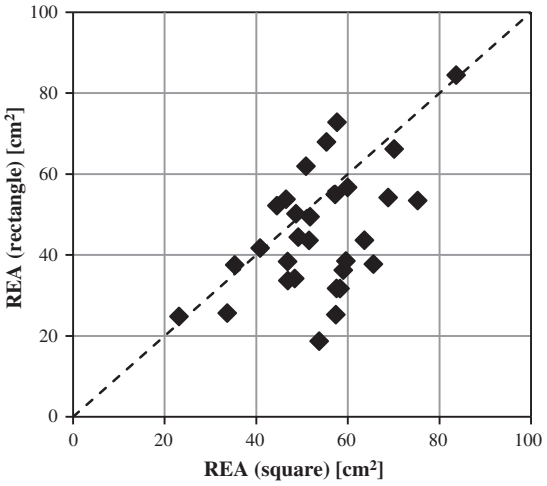


**Fig. 8.** Comparison of REA calculation methods for VPD-89 specimens.

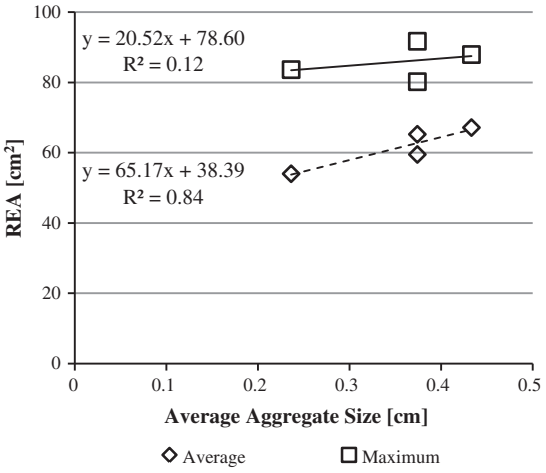


**Fig. 10.** Effect of average particle size on the average and maximum REA.

value as this ensures all the samples are using an area at least as large as their individual REA. Because of this, and the low correlation of the maximum REA values to the porosity (Fig. 10), a constant value for the REA of 83.9 $cm^2$ (13 $in.^2$) was used to smooth the vertical porosity distribution for the samples tested in this study. Only one of the more than 50 faces tested had an REA larger than this for porosities 30% and lower, which is the typical range for porous pavements. Even for the porosities up to 40%, this value is a reasonable maximum that results in little error.

While an REA of 83.9 $cm^2$ (13 $in.^2$) ensures a smooth and accurate distribution of the porosity, the resolution of this profile is very low for an individual sample. For example, a 14.6 cm (5.75 in.) wide face using this REA would require averaging over a 5.7 cm (2.3 in.) deep band. To refine the resolution, multiple specimens can be used to increase the effective width of the sample if they are representative of the same population. For the results presented in this paper, six cylinders were made for each batch which resulted, after cutting, in twelve 14.6 cm (5.75 in.) wide faces. This created an effective width of 175 cm (69.0 in.) which in turn means that the required averaging depth is reduced from 5.7 to 0.5 cm (2.2 to 0.2 in.). Thus the vertical porosity distribution for the mix and compaction method can be found with a much higher resolution.

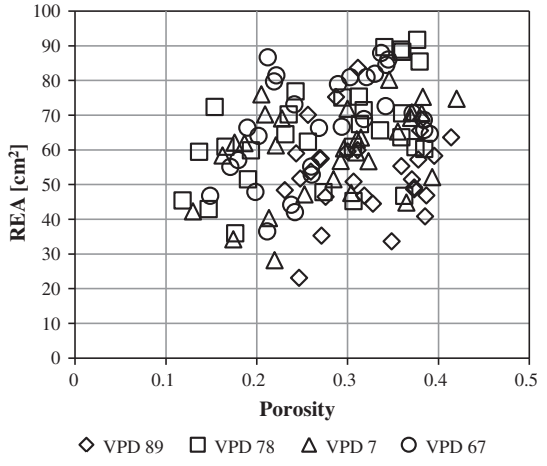


**Fig. 9.** Relationship between REA and porosity.

### 3.3. Sample results for vertical porosity distributions

From the results of the image analysis porosity method, an average vertical porosity distribution was measured for each of the four mixes, using an REA of 83.9 $cm^2$ (13 $in.^2$) and the six samples (12 faces) prepared with each mix. This was compared to the second set of six cylinders which were prepared and cut horizontally into 2.54 cm (1 in.) slices. The porosity of each slice was calculated using the volumetric measurement techniques described in Section 2.2. Additionally, the average areal porosity of each face of the slices was calculated using the image analysis technique. These three data sets are plotted in Fig. 11.

The trend of a relatively low porosity zone just below the open surface texture is clearly visible on all the data sets. Also, at the very top and bottom of the surface, the porosity increases towards 100% as the surface is approached. On the top, the 100% porosity is due to the open surface texture and on the bottom it is due to wall effects. Overall, the image analysis and volumetric measurements agree with each other, with the maximum difference being around 5%.

In addition to the experimental data shown in the figures, an approximate porosity distribution, $P_y$, proposed by Haselbach and Freeman [9] was also plotted. This approximate porosity distribution is given by:

$$P_y = P'\left(1 - \frac{2y}{h}\right) + P\left(\frac{2y}{h}\right) \tag{6}$$

where $P'$ is the un-compacted porosity of the sample (measured from the un-compacted specimens), $P$ is the average porosity of the compacted sample, $y$ is the position, from the bottom, of the sample, and $h$ is the height of the sample.

As can be seen, this is a good approximation for all the mixes except VPD-89. This is because the compaction assumed in the development of Haselbach and Freeman's distribution consists of the specimen being overfilled by a certain height and then compacted to its final height [9]. VPD-89 was the only sample not prepared in this manner and hence, it has the worst agreement with the distribution.

Though Haselbach and Freeman's distribution (6) describes the porosity distribution in the middle of the samples well, the porosity distribution at the ends of the cylinders is poorly described [9].

It is clear that while the porosity distribution generated by image analysis gives the overall trend, there is still some oscillation. This is an artifact of REA being defined as the area which reduces the oscillation in porosity to a range of 5%. To remove this

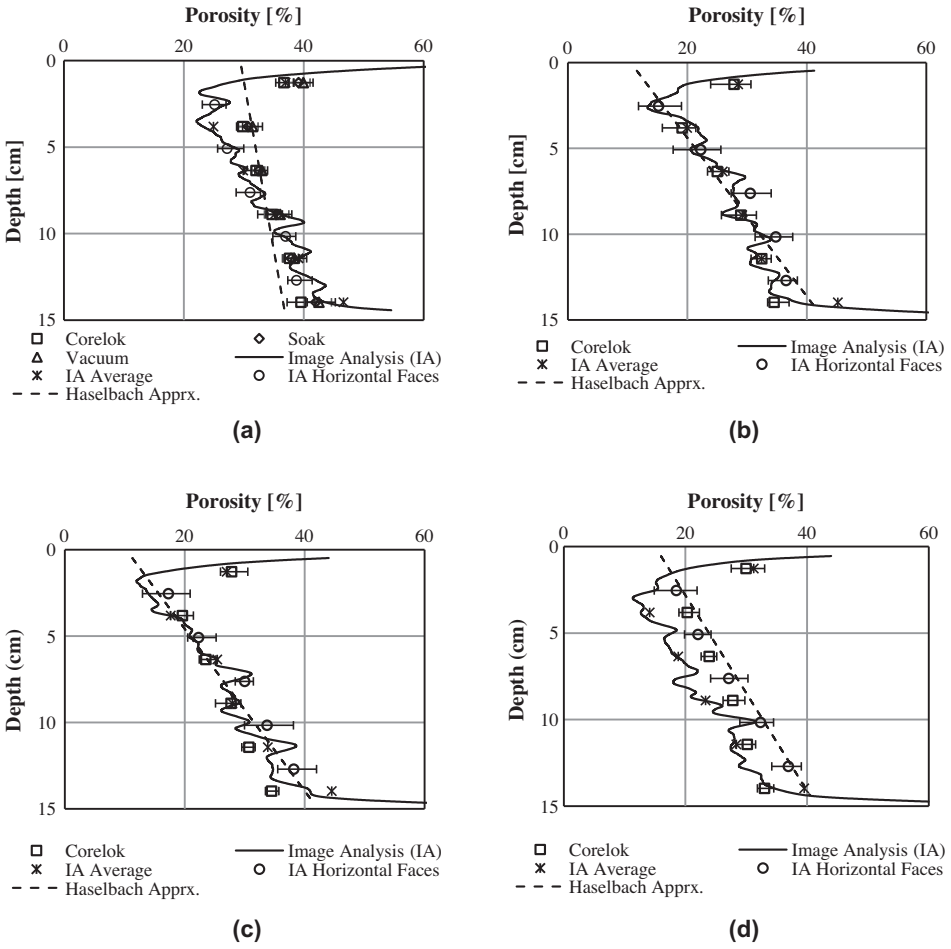


**Fig. 11.** Examples comparing the vertical porosity distribution to average measurements taken at the cut faces and from the slices. The error bars represent the volumetric data's range. Mixes VPD-89, 78, 7, and 67 correspond with (a–d) respectively.

oscillation further, this acceptable range (5%) could be decreased. However, that would increase the REA and either decrease the resolution of the porosity distribution, or require more samples from the population to be scanned and analyzed to keep the same vertical spatial resolution.

## 4. Conclusions

Using image analysis to measure the porosity distribution of a porous pavement has been shown to result in porosity measurements that agree well with existing porosity test procedures. There was shown to be no statistically significant difference between the image analysis measurements and vacuum porosity method when calculating the average porosity, and general agreement by all the methods with respect to the porosity distribution. Further, for the specimens that match the compaction criteria, the vertical porosity distribution measured using the image analysis technique agreed well with the empirical model of Haselbach and Freeman [9] when applied to the interior of the sample.

The REA was identified as an important parameter which enables the raw, individual pixel row porosities to be area averaged to create a smooth porosity distribution with high resolution that is still statistically meaningful. The REA for a sample can be found experimentally using the procedure and definition presented in Sections 2.5.1 and 3.2. For the samples created for this study, an REA of 83.9 $cm^2$ (13 $in.^2$) was experimentally found and used.

Though this process was only used to find the vertical porosity distribution in pervious concrete, it is compatible with other pavement types, such as porous asphalt, and can be used to find distributions in other directions, such as horizontally or radially in cylindrical specimens. Porosity distributions generated using this method are needed to better understand the hydraulic and structural behavior of porous pavement materials, and can be used to study the impacts that non-uniform porosity has on important properties such as hydraulic conductivity, strength and their clogging behavior. This better understanding of the properties of porous pavement can improve design and construction of porous pavements.

## Acknowledgment

The authors would like to thank the Glenn Department of Civil Engineering for their financial support through the CU-SIM program.

## References

[1] American Concrete Institute (ACI). Specification for pervious concrete pavements. MI: Farmington Hills; 2008.
[2] Low K, Harz D, Neithalath N. Statistical characterization of the pore structure of enhanced porosity concretes. In: Concrete technology forum. Focus on, sustainable development; 2008.
[3] Montes F, Haselbach LM. Measuring hydraulic conductivity in pervious concrete. Environ Eng Sci 2006;23:960–9.
[4] Neithalath N. Development and characterization of acoustically efficient cementitious materials. Ph.D. thesis, Purdue University; 2004.
[5] Wang K, Schaefer VR, Kevern JT, Suleiman MT. Development of mix proportion for functional and durable pervious concrete. In: Proceedings of the 2006 NRMCA concrete technology forum—focus on pervious, concrete; 2006.

[6] Putman BJ. Field performance of porous pavements in South Carolina. In: Proceedings of the 2010 South Carolina water resources conference, Columbia, SC; 2010. p. 4.
[7] Mata LA, Leming ML. Vertical distribution of sediments in pervious concrete pavement systems. ACI Mater J 2012;109:149–55.
[8] De Somer M, De Winne E. Method to establish the "porosity-depth" distribution of porous concrete pavement using cylindrical 100 $cm^2$ cores samples. In: Proceedings of the 8th international symposium on concrete roads, AIPCR, Lisbon, Portugal; 1998. p. 171–6.
[9] Haselbach LM, Freeman RM. Vertical porosity distributions in pervious concrete pavement. ACI Mater J 2006;103.
[10] Neithalath N, Sumanasooriya MS, Deo O. Characterizing pore volume, sizes, and connectivity in pervious concretes for permeability prediction. Mater Charact 2010;61:802–13.
[11] Sansalone J, Kuang X, Ranieri V. Permeable pavement as a hydraulic and filtration interface for urban drainage. J Irrig Drain Eng 2008;134:666–74.
[12] Sumanasooriya MS, Neithalath N. Stereology- and morphology-based pore structure descriptors of enhanced porosity (pervious) concretes. ACI Mater J 2009;106:429–38.
[13] ASTM D448 – 12. Standard classification for sizes of aggregate for road and bridge construction. West Conshohocken, PA: ASTM International; 2012.
[14] Putman BJ, Neptune AI. Comparison of test specimen preparation techniques for pervious concrete pavements. Constr Build Mater 2011;25:3480–5.
[15] Rizvi R, Tighe SL, Henderson V, Norris J. Laboratory sample preparation techniques for pervious concrete. In: TRB 88th annual meeting compendium of papers; 2009.
[16] ASTM D7063/D7063M. Standard test method for effective porosity and effective air voids of compacted bituminous paving mixture samples. West Conshohocken, PA: ASTM International; 2011.
[17] Montes F, Valavala S, Haselbach LM. A new test method for porosity measurements of portland cement pervious concrete. J ASTM Int 2005;2:13.
[18] Bear J. Dynamics of fluids in porous media. Courier Dover Publications; 1988.
[19] VandenBygaart A, Protz R. The representative elementary area (REA) in studies of quantitative soil micromorphology. Geoderma 1999;89:333–46.
[20] Haselbach LM, Freeman RM. Effectively estimating in situ porosity of pervious concrete from cores. J ASTM Int 2007;4:100293.